

Dynamical structure of vanishing gradient and overfitting in multi-layer perceptrons

Alex Ali Maleknia^a, Yuzuru Sato^{b,c}

^a*IMAG, IROKO, Univ Montpellier, Inria, CNRS*

^b*Department of Mathematics, Hokkaido University, Kita 12 Nishi 7, Kita-ku, Sapporo, Hokkaido 060-0812, Japan*

^c*RIES, Hokkaido University, Kita 12 Nishi 7, Kita-ku, Sapporo, Hokkaido 060-0812, Japan*

Abstract

Vanishing gradient and overfitting are two of the most extensively studied problems in the literature about machine learning. However, they are frequently considered in some asymptotic setting, which obscure the underlying dynamical mechanisms responsible for their emergence. In this paper, we aim to provide a clear dynamical description of learning in multi-layer perceptrons. To this end, we introduce a minimal model, inspired by studies by Fukumizu and Amari, to investigate vanishing gradients and overfitting in MLPs trained via gradient descent. Within this model, we show that the learning dynamics may pass through plateau regions and near-optimal regions during training, both of which consist of saddle structures, before ultimately converging to the overfitting region. Under suitable conditions on the training dataset, we prove that, with high probability, the overfitting region collapses to a single attractor modulo symmetry, which corresponds to the overfitting. Moreover, we show that any MLP trained on a finite noisy dataset cannot converge to the theoretical optimum and instead necessarily converges to an overfitting solution.

Keywords: multi-layer perceptrons, gradient descent, vanishing gradient, overfitting

1. Introduction

Over the past two decades, significant effort has been devoted to enhancing gradient-based training methods for neural networks [1, 2, 3, 4]. Here, we aim to analyse a minimal dynamical scenario that captures the mechanisms behind two central issues: the vanishing gradient problem and overfitting in gradient descent for multi-layer perceptrons. Motivated by the works of [5, 6, 7], we employ a Fukumizu–Amari model with observational noise in data. Within this setting, the learning dynamics can be described and analysed from a dynamical systems perspective. The theoretical analysis culminates in Theorem 3.1, which asserts that, except for a set of measure zero, and with high probability, every trajectory converges to overfitted solutions when the number of data points

Email addresses: alex.maleknia@inria.fr (Alex Ali Maleknia), ysato@math.sci.hokudai.ac.jp (Yuzuru Sato)

is sufficiently large or the variance of the training data is sufficiently small. We further conjecture that, during the transient dynamics, the system visits numerous saddles, including plateaus and optimal solutions.

The structure of the paper is as follows. After introducing the general notation and definitions in Section 2, we present the main theoretical analysis concerning the overfitting region and the optimal region in Section 3. To complement the analysis, Section 4 provides numerical experiments conducted within the minimal gradient descent model. The purpose is to illustrate the vanishing gradient phenomenon and overfitting in their essential forms. The final section summarizes the results and outlines directions for future research.

2. Preliminaries

2.1. Gradient descent for multi-layer perceptrons

A *multi-layer perceptron* (MLP) [8, 9] consists of a system of interconnected nodes (called *neurons*), typically represented as a computational graph, as illustrated in Fig. 1.

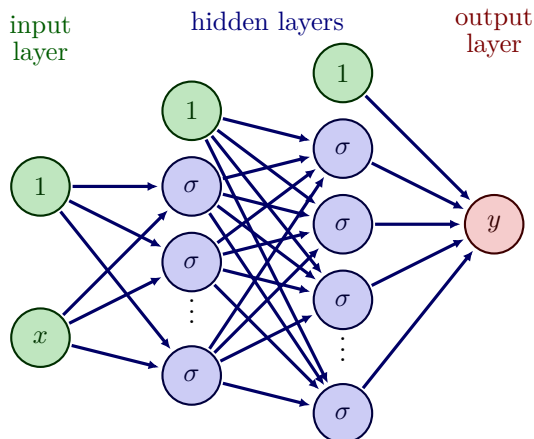


Figure 1: A multi-layer perceptron with two hidden layers of arbitrary size.

An MLP \mathcal{N} naturally defines a function $f_{\mathcal{N}} : \mathbb{R}^{d_{in}} \rightarrow \mathbb{R}^{d_{out}}$, which depends on the architecture, the activation function $\sigma : \mathbb{R} \rightarrow \mathbb{R}$, and the weights of the edges of \mathcal{N} .

For the sake of simplicity, we will focus our efforts on the case of networks with only one hidden layer (3-layer perceptrons). In this setting, we will use the following notation:

- m : number of neurons in the hidden layer;
- $\mathbf{w} = (w_{i,j})$: weights connecting the input layer to the hidden layer for $i = 1, \dots, d_{in}, j = 1, \dots, m$
- $\mathbf{v} = (v_{j,k})$: weights connecting the hidden layer to the output layer for $j = 1, \dots, m, k = 1, \dots, d_{out}$;
- $\mathbf{b} = (b_{1,j}, b_{2,k})$: weights of the constant 1 in the first and second layer (called *biases*) for $j = 1, \dots, m, k = 1, \dots, d_{out}$;

- $\boldsymbol{\theta} = (\mathbf{v}, \mathbf{w}, \mathbf{b})$: the parameter of \mathcal{N} ;
- $\Theta_m = \mathbb{R}^{m(d_{in}+d_{out}+1)+d_{out}}$: the space of all possible parameters.

With the above notation, we can write $f_{\mathcal{N}}$ explicitly as:

$$f_{\mathcal{N}}(x) = f(x; \boldsymbol{\theta}) = \sum_{i=1}^m v_i \sigma(w_i \cdot x + b_{1,i}) + b_2.$$

Given a dataset $D^n = \{(x_i, y_i)\}_{i=1}^n$, we want to find the best fitting function for the data among the m -neuron MLP. This problem is equivalent to finding the best parameter $\boldsymbol{\theta} \in \Theta_m$ such that $f(x; \boldsymbol{\theta})$ minimizes the *training error*:

$$L(\boldsymbol{\theta}; D^n) = \frac{1}{2n} \sum_{i=1}^n h^2(x_i, y_i; \boldsymbol{\theta}), \quad (1)$$

where $h(x, y; \boldsymbol{\theta}) = \|f(x; \boldsymbol{\theta}) - y\|_2$.

In order to find the best parameter, we will use the gradient descent algorithm. Fixed an initial condition $\boldsymbol{\theta}_0 \in \Theta_m$, the update rule is:

$$\boldsymbol{\theta}(t+1) = \boldsymbol{\theta}(t) - \eta \nabla_{\boldsymbol{\theta}} L(\boldsymbol{\theta}(t); D^n) \quad (\text{GD})$$

for each $t \in \mathbb{N}$.

2.2. Vanishing gradient

In many settings throughout machine learning [10, 4, 11, 5, 3], it has been observed that the training process of a neural network can be slowed down when the gradient of the loss function remains close to zero for a long period, before suddenly increasing. This phenomenon is referred to as the *vanishing gradient*, and the resulting slow dynamics is known as the *plateau phenomenon*. The underlying causes of this behaviour in the general setting remain unclear. The study reported in [5] shows that, for an MLP with the hyperbolic tangent activation function, one possible cause of the vanishing gradient is that the parameter $\boldsymbol{\theta}$ approaches a *singular region* where the network becomes reducible [6]; that is, the function $f(x; \boldsymbol{\theta})$ can be represented by a strictly smaller network. In addition, they propose a minimal model, which we refer to as the Fukumizu–Amari model, to investigate the plateau phenomenon. This model serves as the main inspiration for our model:

- $d_{in} = d_{out} = 1$;
- $D^n = D^n(T) = \{(x_i, T(x_i))\}_{i=1}^n$ where $T(x) = 2 \tanh(x) - \tanh(4x)$ and it is called *target function*;
- the considered model is a 3-layer, 2-neuron MLP without bias terms, i.e.:

$$f(x; \boldsymbol{\theta}) = v_1 \tanh(w_1 x) + v_2 \tanh(w_2 x).$$

In this same setting, the authors of [7] showed that, when using online learning, for an optimal range of variance of the data sampling, the plateaus are enhanced due to *noise-induced synchronization* [12].

2.3. Overfitting

While the plateau phenomenon is an intrinsic structural problem for neural networks trained with gradient descent, overfitting is more closely related to learning excessive information from the training data. In real-world applications, such unimportant information typically resides in observational noise, which was not modelled in the work of Fukumizu and Amari [5]. Thus, we would like to consider a dataset of the form $D = D_\tau^n(\omega; T) = \{(x_i(\omega), y_i(\omega))\}_{i=1}^n$, in which, given $\omega \in \Omega$ probability space:

$$\begin{aligned} x_i &\stackrel{\text{i.i.d.}}{\sim} \rho \text{ (probability distribution on } \mathbb{R}^{d_{in}}); \\ y_i(\omega) &= T(x_i(\omega)) + \xi_i(\omega); \\ \xi_i &\stackrel{\text{i.i.d.}}{\sim} \mathcal{N}(0, \tau^2) \text{ (observational Gaussian noise)}. \end{aligned}$$

When a target function T is given, we can define the *generalization error* as:

$$R(\theta; T) = \|f(x; \theta) - T(x)\|_{L^2(\rho)}^2 = \int_{\mathbb{R}^{d_{in}}} (f(x; \theta) - T(x))^2 \rho(x) dx. \quad (2)$$

Note that:

$$\lim_{n \rightarrow \infty} \lim_{\tau \rightarrow 0} L(\theta; D_\tau^n(\omega, T)) = R(\theta; T) \quad (3)$$

for any $\omega \in \Omega$, $\theta \in \Theta_m$.

Introducing observational noise into the dataset leads to the problem of overfitting, which occurs when the model learns the noise in the data rather than the underlying structure of the target function and fails generalization. In other words, during the training process the generalization error may increase while the training error continues to decrease. In fact, even if our goal is to minimize R , we can only compute L , which depends on the dataset D and therefore carries an intrinsic error that makes the learning trajectory deviate from the optimal one.

3. Generic Analysis

For the sake of simplicity, let us assume $\sigma = \tanh$, $\tau > 0$, and T is an MLP of the form:

$$T(x) = \sum_{i=1}^{m^*} v_i^* \tanh(w_i^* \cdot x + b_{1,i}^*) + b_2^*,$$

where $w_l^* \neq w_j^* \neq 0$ for each $l, j = 1, \dots, m^*$, $l \neq j$.

To study vanishing gradients and overfitting rigorously, the first step is to define the objects of our analysis more formally.

Definition 1. *The **optimal region** is the set of parameters that minimizes the generalization error:*

$$\mathcal{M}_m = \{\theta \in \Theta_m \mid R(\theta; T) = 0\}.$$

Definition 2. *We call **overfitting region** the set of parameters that minimizes the training error:*

$$\mathcal{O}_m = \arg \min_{\theta \in \Theta_m} L(\theta; D).$$

Note that \mathcal{M}_m is fixed once the target function T and the number of neurons m are specified. On the other hand, \mathcal{O}_m strongly depends on the dataset, and even when averaged over all possible finite datasets, it still varies with the variance τ of the observational noise. For $\tau = 0$, it is clear that $\mathcal{M}_m \subseteq \mathcal{O}_m = \{\boldsymbol{\theta} \in \Theta_m \mid L(\boldsymbol{\theta}; D_0^n) = 0\}$. However, for any $\tau > 0$, we have $\mathcal{M}_m \cap \mathcal{O}_m = \emptyset$ almost surely, as shown in the following proposition.

Proposition 3.1. *For every $m \geq m^*$, \mathcal{M}_m does not contain any critical points of L for almost every realization of the data noise vector $\xi = (\xi_1, \dots, \xi_n)$. Moreover, L is constant over \mathcal{M}_m and follows the distribution $\frac{\tau^2}{2n}\chi^2(n)$.*

Proof. Let us rewrite the empirical risk as:

$$L(\boldsymbol{\theta}; D) = \frac{1}{2n} \sum_{i=1}^n (f(x_i; \boldsymbol{\theta}) - T(x_i) - \xi_i(\omega))^2. \quad (4)$$

Taking the derivative of (4) with respect to $\boldsymbol{\theta}$ yields:

$$\nabla_{\boldsymbol{\theta}} L(\boldsymbol{\theta}; D) = \frac{1}{n} \sum_{i=1}^n (f(x_i; \boldsymbol{\theta}) - T(x_i) - \xi_i(\omega)) \nabla_{\boldsymbol{\theta}} f(x_i; \boldsymbol{\theta}). \quad (5)$$

If we take $\boldsymbol{\theta}^* \in \mathcal{M}$ and substitute in (5), we get:

$$\nabla_{\boldsymbol{\theta}} L(\boldsymbol{\theta}; D)|_{\boldsymbol{\theta}=\boldsymbol{\theta}^*} = \frac{1}{n} \sum_{i=1}^n (T(x_i) - T(x_i) - \xi_i(\omega)) \nabla_{\boldsymbol{\theta}} f(x_i; \boldsymbol{\theta}). \quad (6)$$

Since $\xi_i \sim \mathcal{N}(0, \tau^2)$, almost surely $\xi_i \neq 0$ for every $i = 1, \dots, n$. Recalling that the derivative of the hyperbolic tangent is always positive, it holds that $\nabla_{\boldsymbol{\theta}} L(\boldsymbol{\theta}; D) \neq 0$ a.s. for all $\boldsymbol{\theta} \in \mathcal{M}_m$, so the points in \mathcal{M}_m cannot be critical points for L . In addition, from (4), one can observe that $L(\boldsymbol{\theta}; D_{\tau}^n(\cdot)) \sim \frac{\tau^2}{2n}\chi^2(n)$ for every $\boldsymbol{\theta} \in \mathcal{M}_m$. \square

An interpretation of the previous result is that, once observational noise is introduced, even if the data-generating mechanism is known, the resulting learning trajectory becomes unpredictable. Numerical experiments suggest that the training process almost always (up to sets of measure zero) converges to a unique function. However, to the best of our knowledge, the literature provides no theoretical guarantee of convergence in this setting. With the intention of giving a formal statement supporting the experiments, we first want to prove that the gradient descent dynamics always converge in our setting.

Proposition 3.2. *In the Fukumizu-Amari setting, for any initial condition θ_0 there exists a learning step η such that the gradient descent algorithm either converges to a critical point of $L(\boldsymbol{\theta}; D)$ or $\lim_{t \rightarrow \infty} \|\boldsymbol{\theta}_t\| = +\infty$.*

Proof. Referring to [13] (Theorem 3.2), we want to prove that $L(\boldsymbol{\theta})$ satisfies the hypothesis, i.e., it is analytical and exists $\kappa > 0$ for which, for any choice of θ_0 and for any $t > 0$, L satisfies the strong descent condition. In our case, it reads:

$$L(\boldsymbol{\theta}(t)) - L(\boldsymbol{\theta}(t+1)) \geq \kappa \|\nabla_{\boldsymbol{\theta}} L(\boldsymbol{\theta}(t))\| \|\boldsymbol{\theta}(t+1) - \boldsymbol{\theta}(t)\|. \quad (\text{SD})$$

The fact that $L(\boldsymbol{\theta}; D)$ is analytical is clear, since it is a finite sum of analytical functions.

To prove that (SD) is true, let us first show that the following inequality holds:

$$L(\boldsymbol{\theta}(t)) - L(\boldsymbol{\theta}(t+1)) \geq \kappa\eta \|\nabla_{\boldsymbol{\theta}} L(\boldsymbol{\theta}(t))\|^2. \quad (7)$$

By the properties of the gradient descent algorithm, since L is smooth and $\nabla L(\boldsymbol{\theta}; D)$ is Lipschitz, we can choose small enough η such that at each step the error is lower than the previous iteration. This implies that the left-hand side is always non-negative and it's zero only if $\nabla_{\boldsymbol{\theta}} L(\boldsymbol{\theta}_t) = 0$. Therefore, by choosing a small enough κ , the inequality holds for any $t > 0$. At this point, substituting $\|\boldsymbol{\theta}_{t+1} - \boldsymbol{\theta}_t\| = \eta \|\nabla_{\boldsymbol{\theta}} L(\boldsymbol{\theta}_t)\|$ from (GD) in (7) will conclude the proof. \square

Corollary 3.1. *Assume that $\lim_{t \rightarrow \infty} \|\boldsymbol{\theta}_t\| < +\infty$. Then, the overfitting region is not empty.*

Proof. By contradiction, suppose that L has no minimum points. This means that the dynamics always converges to saddle points, as the gradient descent algorithm cannot converge to maximum points.

Define $\mu > 0$ to be the infimum of L over the saddle points. Let $\varepsilon > 0$ and pick a saddle point $\boldsymbol{\alpha} \in \Theta$ for which $L(\boldsymbol{\alpha}; D) \leq \mu + \varepsilon$. By definition of saddle point, there must be a direction \boldsymbol{r} in which L is decreasing.

Let $\boldsymbol{\beta} \in \{\boldsymbol{\alpha} + a\boldsymbol{r} \mid a \in \mathbb{R}_+\}$ be the parameter that minimizes L . By taking $\varepsilon < \mu - L(\boldsymbol{\beta}; D)$, we have that if the gradient descent iteration is started from $\boldsymbol{\beta}$ we cannot converge to any saddle point. In fact, $L(\boldsymbol{\theta}(t))$ is non-increasing in t for small enough η [9]. However, by Proposition 3.2, the algorithm has to converge to a critical point, but since μ was the infimum achieved by the training error on saddle points, this critical point must be a minimum. \square

Note that if, instead of assuming $\lim_{t \rightarrow \infty} \|\boldsymbol{\theta}_t\| < +\infty$, one assumes that Θ_m is compact, the result from Corollary 3.1 is trivial: L is a continuous function over a compact set and therefore there exists at least one minimum point.

The next theorem shows that, in a certain sense, the minimum point is unique.

Theorem 3.1. *Assume $m(d_{in} + d_{out} + 1) + d_{out} \leq n$ and $\lim_{t \rightarrow \infty} \|\boldsymbol{\theta}_t\| < +\infty$. Then, for almost every realization of the noise vector ξ , there exists $r > 0$ such that, with probability $1 - \exp(-\frac{r}{\tau} - \sqrt{n})^2/2$, \mathcal{O}_m consists of a single point up to the finite symmetry group generated by $(v_i, w_i) \mapsto (-v_i, -w_i)$, and neuron permutations.*

Proof. For the sake of simplicity, let us assume $d_{in} = d_{out} = 1$ and $\boldsymbol{b} = \boldsymbol{b}^* = 0$, so that $\dim \Theta_m = 2m$. In the general case the same computations hold.

Define the parameter-output function $F: \Theta_m \rightarrow \mathbb{R}^n$ as $F(\boldsymbol{\theta}) = (f(x_1; \boldsymbol{\theta}), \dots, f(x_n; \boldsymbol{\theta}))$. The Jacobian matrix of F is:

$$J(\boldsymbol{\theta}) = \begin{bmatrix} \tanh(w_1 x_1) & \cdots & v_m x_1 \operatorname{sech}^2(w_m x_1) \\ \vdots & & \vdots \\ \tanh(w_1 x_n) & \cdots & v_m x_n \operatorname{sech}^2(w_m x_n) \end{bmatrix}.$$

For distinct $\{x_j\}_{j=1}^n$ and generic $\boldsymbol{\theta} \in \Theta_m$, the $2m$ columns are linearly independent when $n \geq 2m$. Hence, $J(\boldsymbol{\theta})$ has full rank $2m$ on a dense open set, so F is

an immersion. Thus $\mathcal{S} = F(\Theta_m)$ is a $2m$ -dimensional embedded real-analytic submanifold of \mathbb{R}^n .

Thanks to [14], we know that for any C^2 submanifold $M \subset \mathbb{R}^d$, there exists a maximal open set $\mathcal{E}(M)$ such that every point $z \in \mathcal{E}(M)$ has a unique nearest point $proj_M(z) \in M$, and the projection $proj_M : \mathcal{E}(M) \rightarrow M$ is C^1 . Namely, it can be proven that there exists a quantity $r > 0$ called *reach* such that each point with distance less than r from M has unique projection. Since F is a smooth embedding, the result holds in our case.

Let us call $y = (y_1, \dots, y_n)$. We can rewrite the risk as:

$$L(\theta) = \frac{1}{2n} \|F(\theta) - y\|^2.$$

By definition of orthogonal projection, the global minimum $\bar{\theta}$ has to be the projection of the data point vector on \mathcal{S} , i.e., $\bar{\theta} \in F^{-1}(proj_{\mathcal{S}}(y))$. In fact,

$$\min_{\theta \in \Theta_m} L(\theta) = \frac{1}{2n} \min_{\theta \in \Theta_m} \|F(\theta) - y\|^2 = \frac{1}{2n} \min_{s \in \mathcal{S}} \|s - y\|^2,$$

which is achieved by the projection of y on \mathcal{S} (we have proven in Corollary (3.1) that L has minimum over Θ_m).

Note that, in this view, we can rewrite $y = F(\theta^*) + \xi$ where. Therefore, we can say that if $\|\xi\| \leq r$, then $y \in \mathcal{E}(\mathcal{S})$ and it is well defined $proj_{\mathcal{S}}(y) = s^*$. Since $\xi \sim \mathcal{N}(0, \tau^2 Id(n))$, we know from the Gaussian tails bound that

$$\mathbb{P}[\|\xi\| < r] \geq 1 - \exp(-(\frac{r}{\tau} - \sqrt{n})^2/2),$$

which goes to 1 for $\tau \rightarrow 0$ or $n \rightarrow \infty$.

To conclude, we only need to show that $F^{-1}(s^*)$ is unique up to symmetries. To this aim, recall that F fixes the value of $f(\cdot; \theta)$ in $n \geq 2m$ points, therefore by the interpolation theory we can say that $f(\cdot; \theta)$ is unique. Using the results from [15], the fact that $f(\cdot; \theta)$ is unique directly implies that the parameter θ is also unique up to neuron symmetries and transformations of the form $(v_i, w_i) \mapsto (-v_i, -w_i)$. \square

In our vision, it is beyond the scope of this article to discuss precise probability estimates for the previous theorem. However, general bounds for the reach can be found in [16].

One interpretation of this result is that, under certain conditions (that can be achieved, for example, by choosing small data noise variance or a large sample set), up to a measure zero set (to be specified below) every initial condition will converge to an overfitting point, which is unique if we consider the space of functions.

To better clarify what this negligible set is and to give more insights about the transient dynamics that appear during the training, let us recall an important statement from [6]:

Theorem 3.2 (Simsek et al. (2021)). *For an irreducible critical point (for L) $\theta_r^* \in \Theta_r$, the set*

$$\bar{\Theta}_{r \rightarrow m}(\theta_r^*)$$

is a union of $G(r, m)$ distinct, non-intersecting affine subspaces of dimension $m - r$ and all points in $\bar{\Theta}_{r \rightarrow m}(\theta_r^)$ are critical points of L .*

Moreover, for C^2 functions h and σ , if θ_r^* is a strict saddle, then all points in $\bar{\Theta}_{r \rightarrow m}(\theta_r^*)$ are also strict saddles.

In the above citation, a parameter $\alpha \in \Theta_m$ is said to be *irreducible* if there does not exist any $q < m$, $\beta \in \Theta_m$ such that $f(\cdot; \alpha) = f(\cdot; \beta)$. In addition, given $\bar{\theta} \in \mathcal{O}_r$ we define the *symmetry-induced critical points* of $\bar{\theta}$ as:

$$\bar{\Theta}_{r \rightarrow m}(\bar{\theta}) = \{\theta \in \Theta_m \mid f(x; \theta) = f(x; \bar{\theta}) \wedge \theta_i \neq 0 \forall i\}.$$

The measure zero set for which the parameters do not converge to the global minimum is the set of parameters that contain $0 < \mu < m$ *completely synchronized* neurons, i.e., there exist μ pairs of $i \neq j$, $i, j \in [m]$ such that $\theta_i = \theta_j$. In fact, for such neurons the gradient iteration is the same and so they have no chance of separating as time evolves, causing the whole dynamic to live in the subspace $\Theta_{m-\mu}$ (and therefore to converge to $\mathcal{O}_{m-\mu}$).

With the theoretical ground provided by the previous results, we expect that for small data noise variance the learning dynamics, after visiting some saddle points including the plateau regions and the optimal region \mathcal{M}_m , will eventually converge to a point in the overfitting region \mathcal{O}_m , which is a set of pointwise attractors. A schematic view of this saddle–saddle–attractor scenario, representing the trajectory of the parameters, is depicted in Fig. 2.

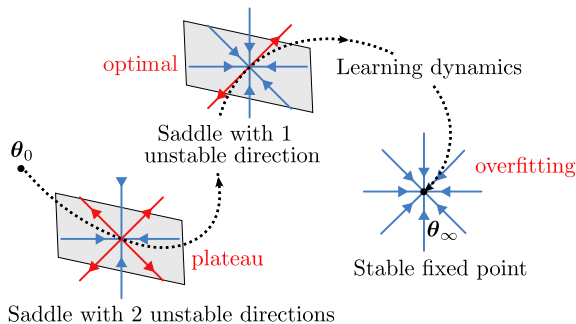


Figure 2: A schematic representation of the saddle–saddle–attractor scenario in MLP gradient descent learning. Empirically, the number of positive eigenvalues is smaller near the optimal region than in the plateau region. The overfitting is a stable attractor.

4. Minimal model and numerical experiments

To confirm the saddle–saddle–attractor scenario illustrated in Fig. 2 through numerical experiments, we propose a minimal MLP model that captures both vanishing gradient and overfitting phenomena. Our idea is to use a modified Fukumizu-Amari model:

- MLP with 1-input, 1-output, 3-layer, 2-neuron without bias;

$$f(x; \theta) = v_1 \tanh(w_1 x) + v_2 \tanh(w_2 x),$$

- Fixed observational noise; $D = D_\tau^n(\omega)$

- Target function; $T(x) = 2 \tanh(x)$;

By means of this model, we will be able to represent the significant dynamics of the learning to give a clear view of the saddle-saddle-attractor scenario. From a dynamical system's perspective, we are focusing on the following 4-dimensional quenched random map:

$$\begin{aligned} w_1(t+1) &= w_1(t) - \frac{\eta v_1(t)}{n} \sum_{i=1}^n \frac{x_i h(x_i, y_i; \boldsymbol{\theta})}{\cosh^2(w_1(t)x_i)}, \\ w_2(t+1) &= w_2(t) - \frac{\eta v_2(t)}{n} \sum_{i=1}^n \frac{x_i h(x_i, y_i; \boldsymbol{\theta})}{\cosh^2(w_2(t)x_i)}, \\ v_1(t+1) &= v_1(t) - \frac{\eta}{n} \sum_{i=1}^n \tanh(w_1(t)x_i) h(x_i, y_i; \boldsymbol{\theta}), \\ v_2(t+1) &= v_2(t) - \frac{\eta}{n} \sum_{i=1}^n \tanh(w_2(t)x_i) h(x_i, y_i; \boldsymbol{\theta}). \end{aligned}$$

where $h(x, y; \boldsymbol{\theta}) = \|f(x; \boldsymbol{\theta}) - y\|_2$ and $D = \{(x_i, y_i)\}_{i=1}^n$.

Note that in this simple setting we know that the singular region producing plateaus is: $\bar{\Theta}_{0 \rightarrow 2}(0) \cup \bar{\Theta}_{1 \rightarrow 2}(\mathcal{O}_1)$ and the optimal region is the embedding of T in Θ_2 .

4.1. Numerical experiments

In the following, we will present numerical evidence to support the theoretical view presented in Figure 2 by running experiments in our minimal setting. The first step is to generate 100 data points x_i sampled from $\rho \equiv \mathcal{N}(0, 1)$. These points will be used to construct two training sets: D_0^{100} and $D_{0.2}^{100}$. Using these data and the 4-dimensional map presented above, we run gradient descent until $t = 2 \times 10^6$. For these choices of τ and n , empirically we are under the hypothesis of Theorem 3.1, therefore we always converge to the same function at the end of the training. Figure 3 presents the results of training on both dataset: in the learning curve, we represent the evolution of both training and generalization error as functions of the training time in a log-log scale; the other plot represents the trajectories of the parameters in Θ_2 . Indeed, we observe that the learning dynamics resemble the scenario illustrated in Fig. 2: the parameters first pass near the singular region, producing a plateau in the learning curve; they then move toward the optimal parameters, where the evolution slows down again. In the end, however, they escape the near-optimal state to finally converge to the overfitting point. Note that, other than the point to which we are trying to converge, we can observe another difference between the experiments run on D_0^{100} and $D_{0.2}^{100}$, which is that in the noisy case the training error remains flat after reaching the near-optimum, whereas when $\tau = 0$ the descent speeds up again. As reported in [17], we can also see that if we compare the noisy case with the perfect-fit data scenario, the first part of the dynamic is almost the same. Therefore, we have confirmation that the noise is learned at last during the training phase and that it is the cause of the overfitting. We have also explored the richer case where T has 2 neurons and $\boldsymbol{\theta} \in \Theta_4$. In such a scenario, we have had the same scheme mimicking Figure 2, but in addition, we have carried out a more generalized numerical analysis, also considering the

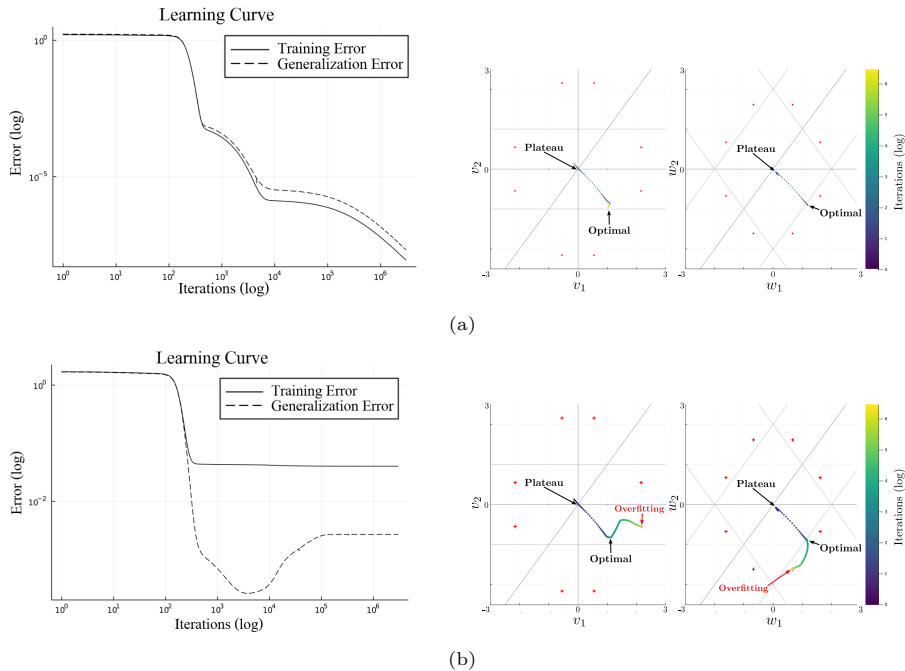


Figure 3: Graphs obtained after training the minimal model for 2 million iterations. In the first column we represent the learning curve; on the right there is a representation of the parameters' orbits during the training, where red stars are the overfitting points and grey lines model the singular region (dark grey) and optimal region (light gray). Plots in (a) represent the training without observational noise (i.e., $\tau = 0$), while in (b) we added some small noise with $\tau = 0.2$.

online learning algorithm and the study of eigenvalues. We suspect that the near-optimal singular region has the least number of escaping directions among the degenerated subspaces. Also, the minimal case scenario shows the same trend: when computing the eigenvalues of the Hessian of the training error on 10^5 points across the plateau region, we get 2 positive eigenvalues. The same experiments, carried out across the optimal region, showed that on those points the hessian has only 1 positive eigenvalue.

5. Conclusion

The problems of vanishing gradients and overfitting in neural networks are often discussed in very complex settings, where the underlying mechanisms remain unclear. However, we believe that the most effective way to address such phenomena is to first understand them in a simplified framework by eliminating extraneous factors that may obscure the essential mechanisms. In this paper, Section 4 introduces a minimal multi-layer perceptron model with two neurons and no bias terms, which exhibits both plateaus and overfitting while attempting to approximate a one-neuron MLP from noisy observations. Furthermore, starting from this almost trivial setting, we prove in Section 3 that, under mild hypotheses, the nonlinear learning dynamics converge almost surely to a point that is unique up to the symmetries intrinsic to tanh networks. Another result

illustrated in Fig. 3 is that the stability of the optimal region changes in the presence of noise in the training data. When the observations are exact, the parameters representing the target function are attractors of the learning dynamics. However, once the noise variance τ becomes positive, this set turns into a saddle. Empirically, these saddles appear to be more attracting than those associated with other singular regions, which gives the saddle-saddle-attractor scenario.

Despite being set in a simple framework, our research is far from exhaustive, and many questions still remain unanswered. For instance, it could be interesting to provide more precise conditions for the uniqueness stated in Theorem 3.1 in order to know a priori if a given network has a unique minimum or not. Another question one could ask is to formulate estimates for the distance δ between the optimal region and the singular region as a function of τ , with the goal of moving the parameters obtained after early stopping within a ball of radius δ to search for real-optimal parameters.

Acknowledgements

Authors thank Professor Andrea Agazzi and Mr. Taichi Yano. The research leading to these results has been partially funded by the Grant in-Aid for Scientific Research (B) No. 21H01002, JSPS, Japan.

Declaration of competing interest

The authors declare that they have no known competing financial interests or personal relationships that could have appeared to influence the work reported in this paper.

CRedit authorship contribution statement

Alex Ali Maleknia: Writing – original draft, Software, Investigation, Formal analysis, Data curation. **Yuzuru Sato:** Writing – review & editing, Validation, Investigation, Funding acquisition, Conceptualization.

Research data

All the necessary tools and information to reproduce the experiments presented in this article can be found at: <https://github.com/alexmare2/Dynamical-structure-of-MLP-with-overfitting>.

References

- [1] D. P. Kingma, J. Ba, Adam: A method for stochastic optimization, CoRR abs/1412.6980.
URL <https://api.semanticscholar.org/CorpusID:6628106>
- [2] K. Jordan, Y. Jin, V. Boza, J. You, F. Cesista, L. Newhouse, J. Bernstein, Muon: An optimizer for hidden layers in neural networks (2024).
URL <https://kellerjordan.github.io/posts/muon/>

- [3] Z. Hu, J. ZHANG, Y. Ge, Handling vanishing gradient problem using artificial derivative, *IEEE Access PP* (2021) 1–1. doi:10.1109/ACCESS.2021.3054915.
- [4] M. Ainsworth, Y. Shin, Plateau phenomenon in gradient descent training of relu networks: Explanation, quantification, and avoidance, *SIAM Journal on Scientific Computing* 43 (5) (2021) A3438–A3468. doi:10.1137/20M1353010.
URL <https://doi.org/10.1137/20M1353010>
- [5] K. Fukumizu, S. Amari, Local minima and plateaus in hierarchical structures of multilayer perceptrons, *Neural Networks* 13 (3) (2000) 317–327. doi:[https://doi.org/10.1016/S0893-6080\(00\)00009-5](https://doi.org/10.1016/S0893-6080(00)00009-5).
URL <https://www.sciencedirect.com/science/article/pii/S0893608000000095>
- [6] B. Simsek, F. Ged, A. Jacot, F. Spadaro, C. Hongler, W. Gerstner, J. Brea, Geometry of the loss landscape in overparameterized neural networks: Symmetries and invariances, in: M. Meila, T. Zhang (Eds.), *Proceedings of the 38th International Conference on Machine Learning*, Vol. 139 of *Proceedings of Machine Learning Research*, PMLR, 2021, pp. 9722–9732.
- [7] Y. Sato, D. Tsutsui, A. Fujiwara, Noise-induced degeneration in on-line learning, *Physica D: Nonlinear Phenomena* 430 (2022) 133095. doi:<https://doi.org/10.1016/j.physd.2021.133095>.
URL <https://www.sciencedirect.com/science/article/pii/S0167278921002505>
- [8] M. A. Nielsen, *Neural Networks and Deep Learning*, Determination Press, 2015.
- [9] C. M. Bishop, *Pattern Recognition and Machine Learning (Information Science and Statistics)*, Springer-Verlag, Berlin, Heidelberg, 2006.
- [10] R. Pascanu, T. Mikolov, Y. Bengio, On the difficulty of training recurrent neural networks, in: S. Dasgupta, D. McAllester (Eds.), *Proceedings of the 30th International Conference on Machine Learning*, Vol. 28 of *Proceedings of Machine Learning Research*, PMLR, Atlanta, Georgia, USA, 2013, pp. 1310–1318.
URL <https://proceedings.mlr.press/v28/pascanu13.html>
- [11] R. Berthier, A. Montanari, K. Zhou, Learning time-scales in two-layers neural networks, *Foundations of Computational Mathematics* doi:<https://doi.org/10.1007/s10208-024-09664-9>.
- [12] J.-n. Teramae, D. Tanaka, Robustness of the noise-induced phase synchronization in a general class of limit cycle oscillators, *Phys. Rev. Lett.* 93 (2004) 204103. doi:10.1103/PhysRevLett.93.204103.
URL <https://link.aps.org/doi/10.1103/PhysRevLett.93.204103>
- [13] P. Absil, R. Mahony, B. Andrews, Convergence of the iterates of descent methods for analytic cost functions, *SIAM Journal on Optimization* 16 (2) (2005) 531–547. doi:10.1137/040605266.

- [14] G. Leobacher, A. Steinicke, Existence, uniqueness and regularity of the projection onto differentiable manifolds, *Annals of Global Analysis and Geometry* 60 (3) (2021) 559–587. doi:10.1007/s10455-021-09788-z.
URL <https://doi.org/10.1007/s10455-021-09788-z>
- [15] A. M. Chen, H.-m. Lu, R. Hecht-Nielsen, On the geometry of feedforward neural network error surfaces, *Neural Computation* 5 (6) (1993) 910–927. doi:10.1162/neco.1993.5.6.910.
- [16] E. Aamari, J. Kim, F. Chazal, B. Michel, A. Rinaldo, L. Wasserman, Estimating the reach of a manifold, *Electronic Journal of Statistics* 13 (1) (2019) 1359 – 1399. doi:10.1214/19-EJS1551.
URL <https://doi.org/10.1214/19-EJS1551>
- [17] N. Rahaman, A. Baratin, D. Arpit, F. Draxler, M. Lin, F. Hamprecht, Y. Bengio, A. Courville, On the spectral bias of neural networks, in: K. Chaudhuri, R. Salakhutdinov (Eds.), *Proceedings of the 36th International Conference on Machine Learning*, Vol. 97 of *Proceedings of Machine Learning Research*, PMLR, 2019, pp. 5301–5310.
URL <https://proceedings.mlr.press/v97/rahaman19a.html>